AD_____

CONTRACT NUMBER: DAMD17-93-C-3086

TITLE: Early Detection of Breast Cancer and Recurrence Following Therapy with Magnetic Resonance Imaging and Spectroscopy

PRINCIPAL INVESTIGATOR: Lawrence Solin, M.D.
Robert E. Lenkinski, Ph.D.

CONTRACTING ORGANIZATION: University of Pennsylvania
Philadelphia, PA 19104

REPORT DATE: April 1996

TYPE OF REPORT: Annual

PREPARED FOR: Commander
U.S. Army Medical Research and Materiel Command
Fort Detrick, Frederick, MD 21702-5012

DISTRIBUTION STATEMENT: Approved for public release;
distribution unlimited

REPORT DOCUMENTATION PAGE

Form Approved
OMB No. 0704-0188

1. AGENCY USE ONLY *(Leave blank)*	2. REPORT DATE	3. REPORT TYPE AND DATES COVERED
	April 1996	Annual (March 1995-April 1996)

4. TITLE AND SUBTITLE
Early Detection of Breast Cancer and Recurrence Following Therapy with Magnetic Resonance Imaging and Spectroscopy

5. FUNDING NUMBERS
DAMD17-93-C-3086

6. AUTHOR(S)
Lawrence Solin, M.D.
Robert E. Lenkinski, Ph.D.

7. PERFORMING ORGANIZATION NAME(S) AND ADDRESS(ES)
University of Pennsylvania
Philadelphia, PA 19104

8. PERFORMING ORGANIZATION REPORT NUMBER

9. SPONSORING/MONITORING AGENCY NAME(S) AND ADDRESS(ES)
Commander
U.S. Army Medical Research and Materiel Command
Fort Detrick, MD 21702-5012

10. SPONSORING/MONITORING AGENCY REPORT NUMBER

11. SUPPLEMENTARY NOTES

12a. DISTRIBUTION / AVAILABILITY STATEMENT
Approved for public release; distribution unlimited

12b. DISTRIBUTION CODE

13. ABSTRACT *(Maximum 200*

We have successfully developed a technical approach that can be employed to produce MRS spectra of the breast lesions as small as $(6\ mm)^3$. These methods have been applied to a cohort of 35 patients. Using the presence of choline in the MR spectra as an indicator of malignancy, the postive predictive value is 0.90. This observation indicates that MRS may be employed in several ways. First it may provide a method for the improved distiction between benign and malignant lesions. Second the presence of choline may provide a means for differentiating recurrent tumor from radiation induced fibrosis. Finally, changes in the choline peak may provide a means for assessing response to therapy in patients with locally advanced breast cancer. Each of these three methods merits further investigation. Future directions that this project may take include: 1)MRS studies of breast lesions at 4.0 T, 2) determining the incremental diagnostic efficiency of MRS, and 3) carrying out an analysis of the cost effectiveness of MRS as a diagnostic method.

14. SUBJECT TERMS
Breast Cancer

15. NUMBER OF PAGES
51

16. PRICE CODE

17. SECURITY CLASSIFICATION OF REPORT	18. SECURITY CLASSIFICATION OF THIS PAGE	19. SECURITY CLASSIFICATION OF ABSTRACT	20. LIMITATION OF ABSTRACT
Unclassified	Unclassified	Unclassified	Unlimited

FOREWORD

Opinions, interpretations, conclusions and recommendations are those of the author and are not necessarily endorsed by the US Army.

X Where copyrighted material is quoted, permission has been obtained to use such material.

___ Where material from documents designated for limited distribution is quoted, permission has been obtained to use the material.

X Citations of commercial organizations and trade names in this report do not constitute an official Department of Army endorsement or approval of the products or services of these organizations.

___ In conducting research using animals, the investigator(s) adhered to the "Guide for the Care and Use of Laboratory Animals," prepared by the Committee on Care and Use of Laboratory Animals of the Institute of Laboratory Resources, National Research Council (NIH Publication No. 86-23, Revised 1985).

X For the protection of human subjects, the investigator(s) adhered to policies of applicable Federal Law 45 CFR 46.

___ In conducting research utilizing recombinant DNA technology, the investigator(s) adhered to current guidelines promulgated by the National Institutes of Health.

___ In the conduct of research utilizing recombinant DNA, the investigator(s) adhered to the NIH Guidelines for Research Involving Recombinant DNA Molecules.

___ In the conduct of research involving hazardous organisms, the investigator(s) adhered to the CDC-NIH Guide for Biosafety in Microbiological and Biomedical Laboratories.

Robert Fell 7/26/96

PI - Signature Date

TABLE OF CONTENTS

Annual Report

Early Detection of Breast Cancer and Recurrence Following Therapy with Magnetic Resonance Imaging and Spectroscopy

Robert. E. Lenkinski, Ph.D. ; Lawrence Solin, M.D.,

Principal Investigators

ANNUAL REPORT

Early Detection of Breast Cancer and Recurrence Following Therapy with Magnetic Resonance Imaging and Spectroscopy

Robert. E. Lenkinski, Ph.D.; Lawrence Solin, M.D.,

Principal Investigators

Contract #: DAMD17-93-C-3086

INTRODUCTION

ORIGINAL GOAL OF THE PROJECT

The major goal of this proposal was to characterize breast lesions as either benign or malignant based on a comparison of a number of anatomical, functional and metabolically based Magnetic resonance imaging (MRI) and Magnetic resonance spectroscopy (MRS) parameters. A group of 15 patients per year all of whom met the inclusion criteria for the MRS studies were to be selected from a larger population of women who were undergoing MRI examinations of the breast. All of these women had detailed histopathological studies performed and the diagnosis of benign or malignant was based on the results of these histopathological studies.

Background. The rising incidence of breast cancer has reached epidemic proportions. In a recent National Institutes of Health consensus development conference (June, 1990), it was emphasized that during the 1990's, more than 1.5 million women in the U.S. will be diagnosed with breast cancer and that approximately 30% of them will die of the disease (1). It is estimated that 1 out of every 9 women will develop breast cancer during her lifetime.

In general, the smaller the lesion is at the time of detection, the better the prognosis (2). While it was readily demonstrable that mammography could detect early, clinically occult breast cancers (3), long term studies were needed to show the efficacy of screening as a means of reducing breast cancer mortality.

The beneficial effect of screening mammography was initially shown in a study undertaken by the Health Insurance Plan of New York (HIP), begun in 1963 (4). This study was the first randomized control study to evaluate the efficacy of screening. From the follow-up evaluation 18 years after the start of the study, a 23% reduction in breast cancer mortality was found for the screened population. In the 1970's, the National Cancer Institute in conjunction with the American Cancer Society undertook the Breast Cancer Detection Demonstration Project (BCDDP) in an attempt to show that population screening was feasible (3,5,6). Detection rates for breast cancer were twice as high as in the HIP study due to improvements in technology. Of all the cancers, 88% were seen on mammography, whereas 42% of cases were not palpable and were detected only by mammography. While not a randomized control study, the BCDDP data strongly suggests a substantial mortality reduction for screened women ages 35-74 (7). An ongoing randomized control study in Sweden has shown at least a 40% reduction in breast cancer mortality with screening (8). Dutch case control studies have shown a 50% reduction in breast cancer mortality with screening (9).

Typical screening programs include annual physical examination and mammography, supplemented with self examination. Although controversial, current recommendations suggest a baseline mammogram between the ages of 35-40, a mammogram every 1-2 years between the ages of 40-50, and a mammogram every year after age 50. In our hospital, results of mammograms are reported as: no suspicious findings; probably benign but warrants close follow-up; well defined mass that requires additional evaluation with ultrasound; or suspicious for malignancy, biopsy recommended. The follow-up algorithm for probably benign lesions is an initial follow-up mammogram at a 6 month interval, then yearly mammography for a period of 3 years. When a lesion of concern is identified mammographically, the only non invasive method for tissue characterization is high resolution ultrasound. If the lesion can be shown to be a simple cyst by ultrasound, a biopsy can be averted.

While mammography has clearly become the gold standard in the detection of early, clinically occult breast cancer, it has limitations. First, not all cancers will be detected mammographically. There are several reasons why breast cancers will be missed, but approximately 30-50% of the false negative mammograms are unavoidable, as the tumor does not produce changes visible with current techniques (10).

Perhaps the most significant limitation of mammography is its relatively low specificity. The positive predictive value for biopsies based on mammographically detected abnormalities is approximately 15%-30% (11), similar to the rate for biopsy of palpable abnormalities (20-25%). This low positive predictive value for mammographically detected abnormalities reflects an overlap in the mammographic appearance of benign and malignant lesions. If it is estimated that 150,000 new cases of breast cancer will be diagnosed each year (1), assuming a 25% true positive biopsy rate, approximately 600,000 breast biopsies will be performed to make these diagnoses. The lack of mammographic specificity subjects many women with benign breast disease to unnecessary biopsy. In fact, it has been estimated that the expense of biopsies is the major cost of screening mammography programs, accounting for 32.2% of this cost, slightly more than the cost of the mammograms themselves (12). However, the introduction of needle biopsy is likely to decrease this cost.

One strategy that has been used to decrease the number of benign biopsies is the use of systematic follow-up of carefully selected low suspicion lesions as an alternative to biopsy. Two studies looking at follow-up of these lesions found a very low percentage of malignancy (<1%) in lesions followed closely for 3-3 1/2 years (13, 14). In one study only .5% of the 3,172 low suspicion lesions that were followed for at least 3.5 years were found to be malignant. During the same period of time, 38% of the needle localization biopsies were positive for malignancy, suggesting an improvement in the rate of benign biopsies(14). Judicious follow-up of low suspicion lesions is therefore promising as an alternative to biopsy and can improve the rate of positive biopsies over that previously described in the literature. However, it would be very advantageous to develop additional ways to decrease the number of benign breast biopsies, without compromising our ability to effectively screen for breast cancer.

High resolution ultrasound can characterize some mammographically detected abnormalities by differentiating simple cysts from solid lesions. However, it is not generally considered a technique to characterize solid breast masses. CT scanning has not demonstrated any significant role in the evaluation of patients with suspicious breast lesions (15).

Another potential method to decrease the number of surgical biopsies that result from mammographic screening, is stereotactic fine needle aspiration biopsy (FNAB) (16). There are significant problems associated with this procedure including false negative biopsies (5-14%) and obtaining insufficient tissue (10-26%). In addition, this technique requires a skilled cytopathologist. More recently, core-needle biopsy has received attention as an alternative to FNAB. Although generally felt to be more accurate than FNAB, there are few studies comparing core needle biopsy to surgical biopsy in the same patient population. Four such studies that include a total of 411 patients have reported sensitivities of this technique for cancer from 85-100% (17-19). However, there has been a single report of seeding of the needle tract with tumor following core needle biopsy, raising a potential risk of this technique (20). There remains significant debate relative to the indications for core needle biopsy as a less invasive alternative to surgical biopsy (21).

MRI. Magnetic Resonance Imaging offers exciting potential for increased tissue characterization compared to other imaging modalities. Early reports using MRI to detect both benign and malignant breast lesions suggested that it was not possible to detect and characterize lesions on the basis of signal intensities on T1 and T2 weighted images (22-24). However, reports on the use of gadolinium enhanced breast MRI were more encouraging. Cancers were shown to enhance relative to other breast tissue following the administration of intravenous contrast agent Gadolinium (III) diethylene-triamine-pentaacetic acid (Gd-DTPA) (25). In one MRI study, 20% of cancers were seen only after the administration of Gd-DTPA (26). A potentially important finding in two studies was the MRI diagnosis of breast cancer not visible on mammography (26, 27). The detection of mammographically occult multifocal cancer in up to 30% of patients has led some investigators to recommend its use to stage patients that are candidates for breast conservation therapy (28).

The presence of enhancement alone is not specific for cancer. Fibroadenomas, benign proliferative change and inflammatory change have also demonstrated enhancement after injection of Gd-DTPA. Preliminary results of dynamic examinations that studied the kinetics of enhancement suggested that increased tissue specificity is possible (25-27). In these studies, cancer demonstrated the most intense enhancement, particularly in the initial phases of the contrast bolus. Benign solid tumors such as fibroadenomas were shown to demonstrate variable contrast enhancement, but it appeared to be more delayed than that seen in malignant tumors. In the first minute after contrast injection, cancers were found to have twice the enhancement of fibroadenomas and 4 times the enhancement of normal breast tissue. At times up to 30 minutes after contrast enhancement, benign and malignant tissue demonstrated a similar amount of enhancement (25).

There have been a number of reports on the use of contrast enhanced MRI to distinguish benign from malignant breast lesions. Most investigators have placed a premium on studying the time course of signal intensity changes of a breast lesion after the bolus injection of Gd-chelate. Unfortunately, scan protocols vary widely among the investigators in this area. For example, Boetes et al (29) place a premium on high time resolution. Their protocol consists of single slice non-fat suppressed gradient echo images with 2.6X1.3 mm in plane spatial resolution (10 mm slice) at 2.3 sec. time intervals. They used a criterion that any lesion with visible enhancement in less than 11.5 seconds after arterial enhancement was considered suspicious for cancer. This criteria resulted in 95% sensitivity and 86% specificity for the diagnosis of cancer. A similar single slice technique has been reported by others with a time resolution varying from 6-60 seconds (27,30). Citing problems determining the proper location on the precontrast images to perform a single slice dynamic examination and the need to detect other lesions within the breast, other investigators have recommended a multislice technique that records dynamic data from the entire breast after the injection of contrast (31-35). These investigators have used multislice 2D gradient echo, 3D gradient echo and echo planar techniques with time resolution varying from 12 seconds to 1 minute and widely distributed spatial resolution and section thickness. The use of keyhole imaging techniques that dynamically sample the center of K space after contrast administration has been suggested as a technique to obtain dynamic high resolution 3D images of the entire breast (36). However, the

spatial resolution of the enhanced tissue is limited since only part of K space is sampled after contrast injection. This makes it difficult to assess lesion architecture. Criteria used to differentiate benign from malignant lesions has also varied widely among investigators. Criteria as simple as % enhancement at 2 minutes to physiologic models that take into account the initial T1 of the lesion to calculate Gd concentration as a function of time in order to extract pharmacokinetic parameters have been reported. The accuracy's cited by these investigators for differentiating benign from malignant lesions varies from 66% to 93% (29-36). Despite the many different techniques and results cited above, it is clear that there is a tendency for cancer to enhance more rapidly than benign lesions after the bolus intravenous injection of Gd chelate. However, it is also clear that despite any technique and interpretation criterion used, there is some overlap in the dynamic curves between cancer and benign lesions. This has resulted in false negative diagnoses in all series.

Others have taken an alternative approach to the characterization of enhancing lesions on breast MRI. They have taken advantage of the soft tissue contrast of MRI to extract architectural features that describe breast lesions (37). Some reports (23,34) on the use of the architecture of breast lesions have suggested a limited role for these features in the interpretation of breast MRI. However, using higher spatial resolution techniques others have reported more optimistic results (37,38).

MRS. The applications of MRS to human tumors has been reviewed by Negendank (39). A general finding was elevated levels of phospholipid metabolites such as phosphomonoesters (PME), phosphodiesters (PDE) and choline containing compounds (Cho). Degani et al (40) have reviewed the pre clinical studies of breast cancer. NMR data obtained from P-31 studies carried out on different malignant cell lines and human mammary epithelial cells indicate differences in the phospholipid metabolism of human breast cancer cells either in tissue culture or implanted in nude mice (40). The malignant cells consistently exhibited elevated levels of phosphocholine and phosphoethanolamine (40). The review of Degani et al (40) also describes the results of C-13 NMR studies which compared glucose utilization rates in malignant cell lines with human mammary epithelial cells. These studies indicated that the malignant cells produced ATP almost exclusively by glycolysis (with concomitant production of lactate) whereas

the human mammary epithelial cells had about 20% oxidative metabolism. Degani et al (40) also describe the results of C-13 studies aimed at determining the details of phospholipid metabolism in human breast cancer cells. These results, carried out in spheroids, showed that the rate of synthesis of phophatidylcholine was greatest in cells which were proliferating as compared with non-proliferating cells. These studies provide a rationale for entertaining the hypothesis that breast lesions that are malignant will exhibit altered metabolism when compared with benign lesions.

Sijens et al (41) have reported changes in both H-1 and P-31 MRS in patients (n=5) with breast cancer. The fat to water ratio was found to be 0.45 in the tumors as compared with 3.3 in normal tissue. The tumors showed elevated levels of PME, PDE and inorganic phosphate (Pi). The tumors all showed little or no phosphocreatine (PCr/ATP <0.2). Similar alterations in P-31 spectral parameters have subsequently been reported by others (42-47).

Gribbestad et al (48) have recently reported a one and two dimensional NMR study of perchloric acid extracts of human breast carcinomas. Amongst a number of interesting findings these authors found elevated levels of phosphocholine at 3.2 ppm. The PC/valine ratio in tumors was 18.7 ± 12.5 as compared with 6.60 ± 2.60 for non-involved tissue. These differences were found to be statistically significant ($p<0.01$) on a Mann-Whitney test. It was pointed out that the increase in PC might be accompanied by a decrease in GPC. These authors also reported a higher level of lactate/glucose in extracts of tumors as compared with non-involved tissue. Some caution in the interpretation of lactate levels in extracts is probably warranted since it is often difficult to remove the tissue in a manner that guarantees that agonal metabolism does not produce lactate. The observation of glucose resonances in the extract provides some confidence that this may not have occurred in the study.

von Speckter at al (49) have also reported a high resolution NMR study carried out on 56 cases with suspected mammary carcinoma. These authors found that three ratios of compounds detected by NMR (the creatine/fat, choline/fat and carnitine/fat ratios) could distinguish between malignant and normal tissues at the 0.995 confidence level. The spectra shown in this report suggest that of the

three compounds, the level of choline should be easiest to determine at 1.5 T in vivo.

The results discussed above show that there are differences in the metabolism of breast cancers compared to normal tissue. Moreover these differences can be observed by MRS methods in cellular suspensions, model tumors and extracts of excised human tissue. As part of the technical advances that were made in vivo MRS at 1.5 T as part of this project it is possible to obtain localized ^1H spectra from lesions that are as small as $(6\ mm)^3$ in size in a total of about ten minutes.

Significance. We begin by defining some of the statistical parameters which can be used to assess the clinical utility of a given test. The sensitivity of the test is given by,

$$Sens = TP/(TP+FN) \qquad [1]$$

where TP is the number of true positive results, i.e. subjects who have the disease that the test correctly identifies; and FN is the number of false negatives, i.e. the number of subjects who have the disease that the test incorrectly identifies as disease-free. The specificity of the test is given by,

$$Spec = TN/(TN+FP) \qquad [2]$$

where TN is the number of true negatives results, subjects who are correctly identified as disease-free; and FP is the number of false positive results, the number of subjects who are disease-free who are incorrectly identified as having the disease. The positive predictive value (PPV) is defined as,

$$PPV = TP/(TP+FP) \qquad [3]$$

The negative predictive value (NPV) is defined as,

$$NPV = TN/(TN+FN) \qquad [4]$$

At present, about one of every four women with positive findings on mammography have a biopsy proven malignancy. Although preliminary reports of MRI have shown variable sensitivities and specificities for the diagnosis of disease, MRI appears to have the potential for achieving both higher positive predictive values and negative predictive values than mammography. If the trends observed in our results obtained as part of this study (described in the following section) are valid in a larger patient cohort, it is clear that MRS will play an important role in the characterization of breast lesions either on its own or in combination with MRI.

The prevalence of breast cancer is about 0.4 % in women over the age of forty. This means that there will be more than 100,000 new cases of breast cancer diagnosed every year. These diagnoses are currently being made from the combination of mammography, biopsy and ultrasound for cystic masses. On this basis there are about 300,000 negative biopsies per year. The elimination of the need for a portion of these biopsies can result in a substantial cost savings to the health care system. To date, most economic analyses of breast cancer have focused on screening mammography (50,51) or have considered the cost effectiveness of treatment for breast cancer(52). To our knowledge, only one decision model has analyzed the cost effectiveness of competing workup or staging strategies for breast cancer (53), specifically the potential cost effectiveness of stereotactic core biopsy. There is now substantial data to suggest that high-resolution breast MRS may hold promise for the workup of breast cancer. Specifically, breast MRI has the potential to reduce the number of negative biopsies of benign lesions (54). To our knowledge, no studies have yet examined and modeled the clinical and economic effects of these potential changes.

BODY

Methods.

The development of multicoil MR of the breast. We have developed a multicoil array specifically for imaging the breast. This array has the advantage of eliminating the requirement of accurate coil placement, while providing adequate sensitivity to support high resolution studies. We have three 1.5 Tesla Signa

(General Electric, Milwaukee, Wisc) systems equipped with the multicoil package. This consists of 4 separate NMR receivers, and the software to simultaneously acquire data from 4 separate receive channels. There are connections for up to 6 coils, with the ability to select up to 4 of the 6 coils for image acquisition. The 4 separate images that are acquired by the 4 separate receiver channels are combined together, weighting the data according to the relative signal within the 4 channels in each pixel. This has the effect of maximizing the signal to noise ratio in the composite image, by minimizing noise contributions from channels in areas outside their sensitive volume. The net result is an image that has the spatial coverage of 4 receiver coils, and the signal to noise ratio of that from a single surface coil.

The design for a breast array consists of 4 coils, 2 on either side of the breast. The coils are arranged on a planar surface in the geometry shown in Figure 1. The coil is applied to the breast similar to the compression planes in the medial-lateral oblique mammographic projection. This provides the ability to examine the maximal amount of breast tissue, including the axillary tail. Compression is applied with care taken not to cause patient discomfort. Compression serves several purposes. First, it effectively limits the size of the breast in 1 dimension. This makes it easier to identify the suspicious region of the breast, since the required spatial coverage in the compression dimension is limited. Second, the geometry of the compressed breast is more suitable for surface coil MR imaging. The reduced distance between the surface and the center of the breast allows for the use of smaller coils without the center of the breast being outside the sensitive volume of the coils. Smaller coils provide a higher signal to noise ratio, and thus support higher resolution imaging. The reduced spatial coverage of the smaller coils can be offset by the use of a multicoil array as described above. In addition, gentle compression also holds the breast in a fixed position relative to the coil, therefore fixing the coils stabilized the breast and reduced motion artifacts.

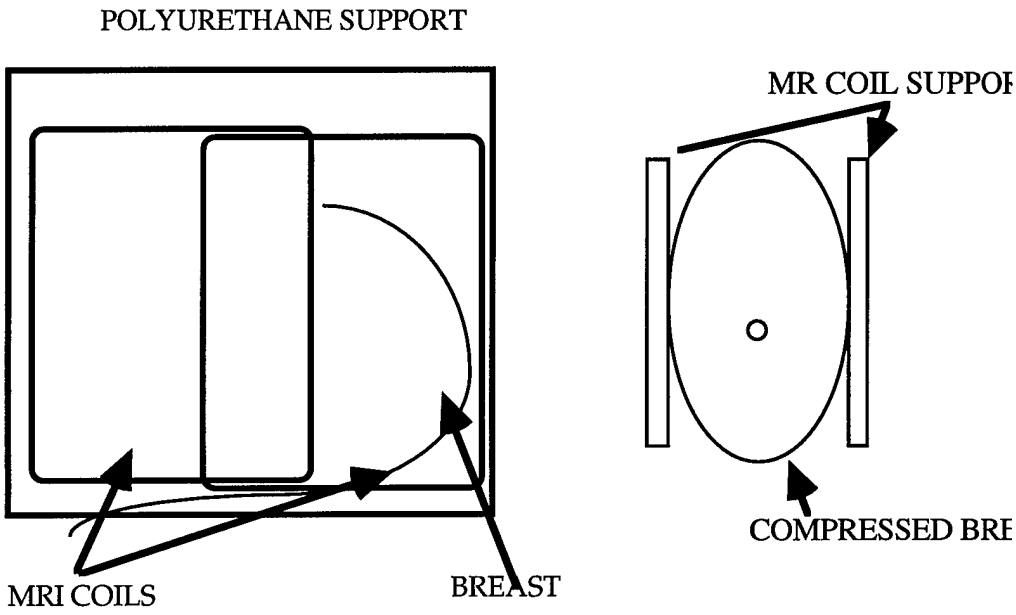

Figure 1. A schematic diagram of the breast multicoil device currently used in our studies.

Patient Selection. 35 patients over 18 years of age and who were referred for breast biopsy for one of the following reasons were recruited into the study:

1. suspicious mammographic finding.
2. clinical suspicion of breast disease.
3. a mass visible on MRI that is at least 1 cm^3 in size.

These patients were selected from a larger study group who are being recruited by Dr. Mitchell D. Schnall from a clinical research protocol which enrolls about 100 cases per year. The ratio of benign to malignant mass found in this population is about 2:1.

Exclusion Criteria:

Patients with a contraindication to MRI examination as well as those who have had a recent (within the past 6 weeks) needle biopsy of the suspicious area were excluded from study. Contraindications to MRI examination include:

1. Medically unstable or hematologic, renal, or hepatic dysfunction
2. Cardiac pacemaker

3. Intracranial clips, metal implants, or external clips within 10 mm of the head
4. Metal in their eyes
5. Pregnant or nursing
6. Claustrophobia

A description of the clinical MRI/MRS protocol employed

MRI. . After obtaining informed consent, the patients were placed prone on the breast imaging platform and the 4 coil array was positioned on the patient. The following MRI sequences were performed:

1. An axial T1 weighted localizer 20 cm field of view (FOV).
2. Sagittal T1 (400/17; 512x384; 18 cm FOV; 3 mm slice thickness) **5 min**
3. Sagittal T2 FSE with fat suppression(4000/80, 512x384; 18 cm FOV; 2 mm slice thickness) **4 min**
4. Sagittal gradient echo dynamic contrast enhancement study with fat suppression (11/2.2; 512x384x32 3D; 35 degree flip angle; 16 cm FOV 2-2.5 mm slice thickness). This scan was performed pre and post injection of 0.1 mM/Kg Gd-DTPA. The sequence was repeated 5 times for a total of 500 sec. **15 min**

The MR images were reviewed by Dr. Mitchell Schnall in order to ascertain the following.

1. The presence of a focal mass observable either prospectively or retrospectively on the precontrast MR sequences which was at least 1 cm^3 in size.
2. The presence of a lesion which was at least 1 cm^3 in size, visible only post contrast administration, and is located close to anatomical features identifiable on precontrast scans.

Subjects who met either of these two criteria were recruited into the MRS protocol.

MRS.

Solvent suppressed proton spectra were obtained using the stimulated echo acquisition mode (STEAM) method by;

1. Selecting the voxel location from the appropriate MR images. (minimum voxel dimensions were 6 mm x 6 mm x 6 mm).
2. Obtaining MR images of the voxel with a TR of 400 msec /TE 16 msec to ensure the correct location of each voxel (the sequence supports this option). This acquisition takes **54 sec.**

3. Employing the automated STEAM acquisition sequence to optimize both the adjustment of the homogeneity as well as the solvent suppression. The resulting FID was stored. This part of the procedure takes **three minutes.**

4. A solvent suppressed spectrum was obtained from the voxel with a TE of 31 msec, and 256 averages per spectrum. This spectrum required about 8 minutes of acquisition

Results Obtained

Improvements in multicoil spectral methods. Multicoils have been used to improve SNR in single voxel proton MR spectroscopy (MRS) and Chemical Shift Imaging (CSI). In order to determine the optimal method for processing multicoil MRS data two recombination schemes were tested using simulations and ^{1}H-MRS data acquired with a 4 channel multicoil. The two methods are computing a simple sum and a weighted sum. In the weighted sum, the contribution of each spectrum to the sum is weighted by its amplitude. In the simple sum, all of the spectra are equally weighted. SNR comparisons are made relative to a reference spectrum obtained from the coil in the array which has the largest amplitude spectrum. Consider the two cases shown in Figures 2 A and 2 B

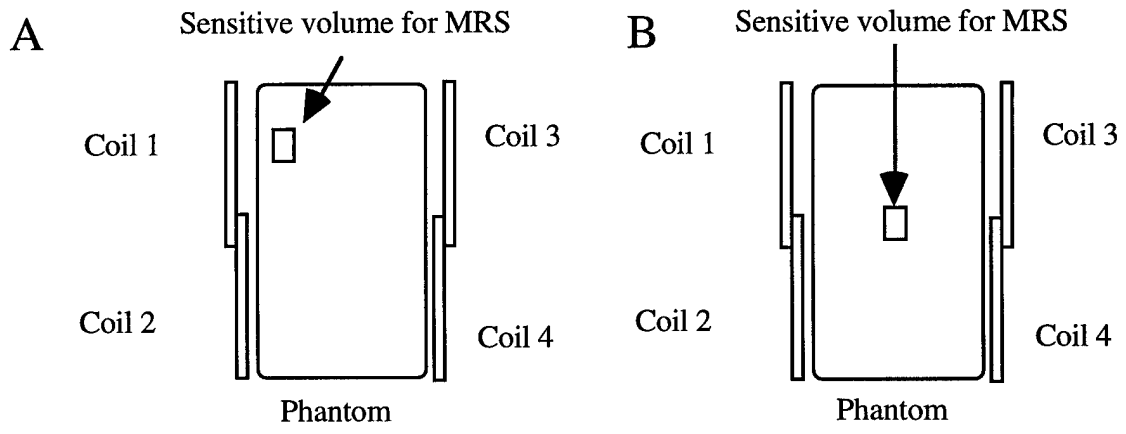

Figure 2. Two examples of voxels placed for localized MRS studies of a phantom. The example shown in A has the voxel placed in the center of the sensitive reception region of coil 1. In B the voxel is placed equidistant from all four of the coils in the multicoil array.

In the example shown in Figure 2 A, the spectrum obtained from coil 1 would contain almost all of the signal, with coils 2-4 containing mostly noise. If the noise is uncorrelated i.e., not the same random noise in each coil then the weighted sum will have preserve the signal-to-noise by minimizing the contribution of noise to the summed spectra. The simple sum will be a less optimal combination since each spectrum is weighted equally. In The example shown in Figure 2 B the spectra obtained from each coil will have the same amplitude. The simple sum and weighted sum are equivalent in this case. In general the weighted sum approach has the advantage when the spectra obtained from the individual coils have unequal amplitudes. The improvement in signal to noise obtained from a four coil multicoil array over a single coil can range from about 20% to a factor of two (squareroot of 4) depending on the location of the sensitive volume for spectroscopy.

An experimental illustration of these theoretical predictions is shown in Figure 3.

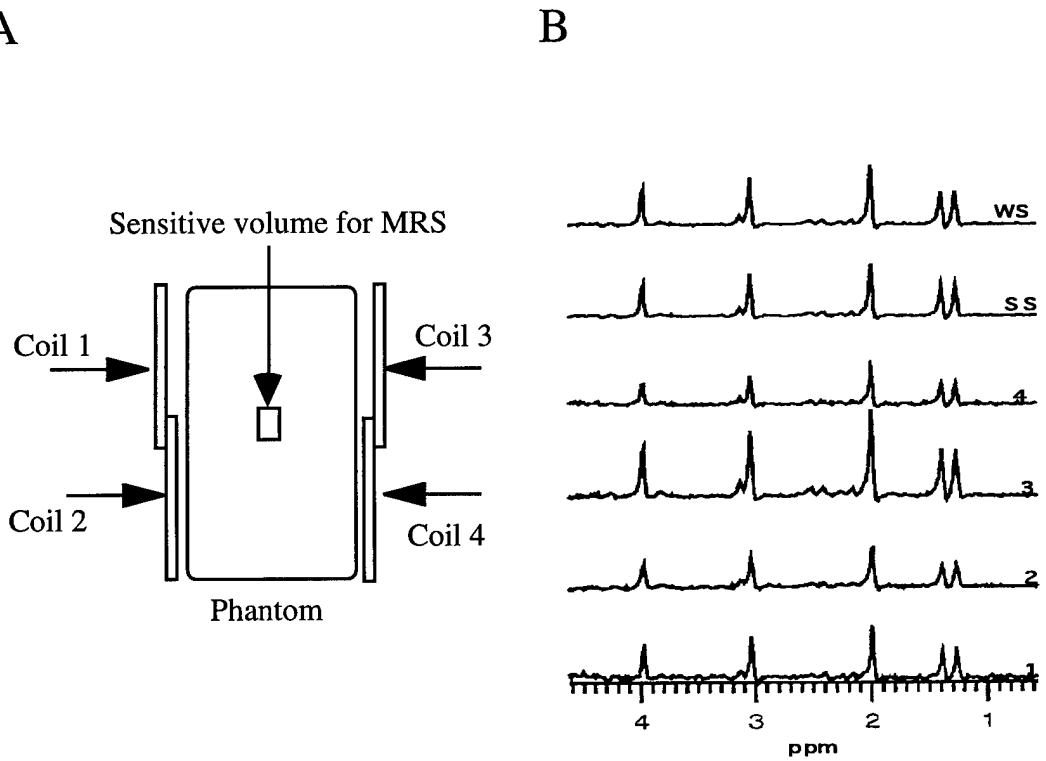

Figure 3. A. A four coil array with the sensitive voxel indicated. **B** Localized MR spectra obtained from the voxel shown in Figure 3 A.

The phantom contained 10 mM creatine, 10 mM N-acetylaspartate and 5 mM glutamine. The arrows show the center of each coil. Coils 1 and 4 are each 8X7 cm while 2 and 3 are 10X4.5 cm. Solvent suppressed spectra (TR 2000, TE 31) were acquired from a $(2\ cm)^3$ voxel at the location shown. The order of the spectra is from bottom to top) is coils 1-4, simple sum, and weighted sum. The signal to noise of the weighted sum was found to be about 20% better than the simple sum in this case. This is because the voxel is approximately equidistant from all four coils. The signal to noise of the weighted sum is a factor of 1.8 times better than the maximum signal to noise of any of the individual coils, confirming the theoretical predictions made on the basis of simulations.

Improved spatial localization for MR spectroscopy. The use of short echo, solvent suppressed localized proton MRS in studies outside the brain have been hampered by contamination of the spectra with resonances arising from lipids which are outside the region of interest. There have been a variety of remedies suggested for this problem. These include applying spatial presaturation pulses prior to executing the localization sequence, improving the spatial selectivity of the Radio Frequency (RF) pulses employed and eliminating contaminating magnetization by using spoiler gradient pulses or phase cycling schemes. These remedies may be used alone or in combination with each other. We wished to determine which single remedy or combination of these remedies can effectively remove lipid contamination. We have constructed a phantom containing two compartments as shown in Figure 4.

A cubic voxel measuring 6 mm per linear dimension was positioned against the inner edge of the phantom containing aqueous solution. Solvent suppressed proton spectra were obtained using the STEAM sequence with an interecho delay (TE) of 31 msec on a General Electric Signa 1.5 T scanner. The study was performed with a breast array (body coil transmit). Solvent suppression was achieved by employing three chemically shift selective (CHESS) pulses before the three slice selective 90 degree STEAM pulses.

Using this phantom we tested three different options for reducing the lipid signal; 1) spatial presaturation (six sided); 2) phase cycling (2 and 8 step) and 3) the use of digitally crafted slice selective pulses (generated with the Shinnar-LeRoux algorithm) with very sharp and less sharp spatial profiles. For the sake of

convenience we refer to these options as 1) sat or no-sat, 2) 2 PC or 8 PC (PC referring to phase cycling), and 3) sharp or fuzzy.

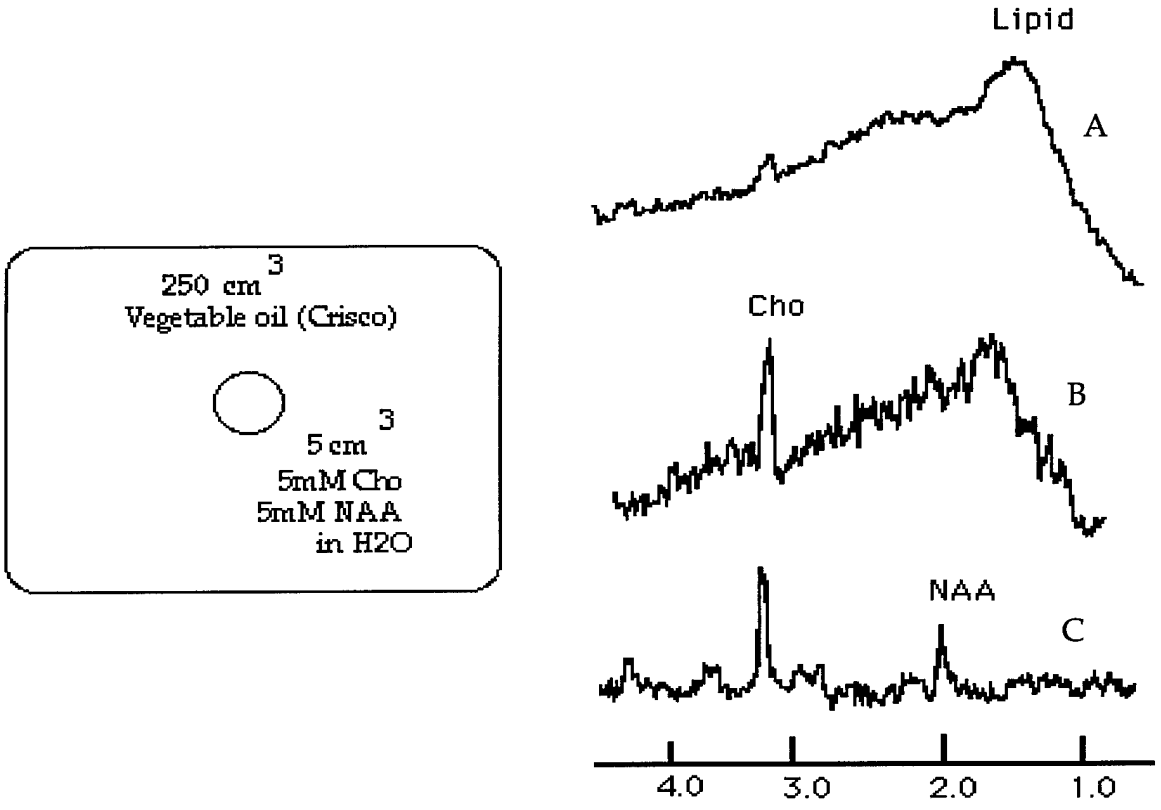

Figure 4. A schematic diagram of the phantom used in the localized MRS studies. The phantom contains N-acetylaspartate (NAA) and choline (Cho). Spectra were obtained with the options indicated in the text.

It is important to note that even the pulses with less well defined spatial transition zones were superior to single lobe sinc pulses. All possible combinations of these options were also evaluated. The use of the sat option reduced the intensity of the lipid peak by about a factor of four. We also found that the use of 8 step phase cycling (8 PC) improved the baseline. Note that the combination of fuzzy, and 2 PC produced a spectrum (spectrum A) with considerable lipid signal. The combination of fuzzy, 2 PC, and no-sat gave a spectrum with reduced lipid signal (spectrum B). The best results were obtained with sharp, 8 PC and sat (spectrum C) although the improvement over sharp, 8 PC and no-sat was minimal.

Our results indicate that the most important factor in reducing lipid contamination is the use of digitally crafted RF pulses with sharp spatial transition zones. These pulses require more time to play out than pulses with broader transition zones. This may mean that the minimum echo delay is somewhat lengthened. For MRS applications in tissues like the breast which contain or reside in fat, the elimination of out of voxel lipid signal is critical in obtaining interpretable solvent suppressed proton at short echo delays.

The spatial precision necessary to acquire MR spectra from (6 mm)^3 voxels. Consider an object of volume, V_{tot}. If we use a spatial localization method to select a smaller volume of this object, V_{sel}, from which we wish to obtain a localized spectrum, then the spatial discrimination, D, of the method can be expressed as:

$$D = [\frac{Vtot - Vsel}{Vsel}] \qquad [5]$$

Under the simplifying assumption of a uniform distribution of metabolites we can define the spatial precision required for a specified level of contamination (S_{sel}/S_{out}) of the spectrum obtained from the selected volume with signal originating from the unselected (V_{tot} -V_{sel}) volume as

$$SP = [\frac{Vtot - Vsel}{Vsel}] \times [\frac{Ssel}{Sout}] \qquad [6]$$

If we assume that the object has a total volume of 1000 cm^3 and the selected volume is 1 cm^3 then from equation 5 the value of D is 999. If we define 10% contamination as acceptable, then the value of SP from equation 6 is about 10^4. From equation 5 it is clear that as the selected volume becomes smaller the spatial precision of the method must become higher.

In order to test spatial precision of the STEAM localization method discussed in the preceding section, we determined the relationship between the peak area to noise and the selected voxel volume in the phantom shown in Figure 5.

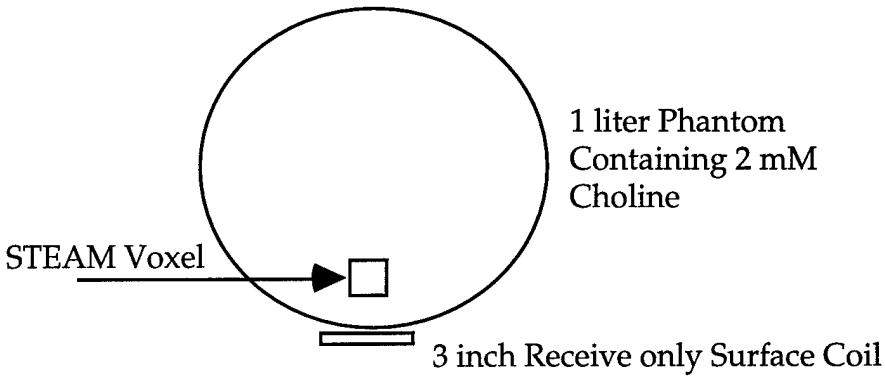

Figure 5. The phantom employed to test the spatial precision of the STEAM method.

Under ideal conditions the relationship between the area to noise and the voxel volume should be a straight line with zero intercept. We experimentally determined this relationship by determining the area to noise of the choline resonance at voxel volumes between 0. 2 and 1.2 cm^3. Since only the gradient strength was varied in the volume selection process, we assumed that the RF pulses had an invariant frequency profile. By analyzing the results of these experiments carried out with the options indicated in Figure 4 we were able to define the fractional contamination as S_{out}/S_{sel}. The results obtained with standard RF pulses (Fuzzy), RF pulses designed for high spatial precision (Sharp) in combination with two and eight step phase cycling schemes are shown in Figure 6.

Our results obtained on phantoms indicate that the STEAM sequence with conventional RF pulses can only achieve values of spatial precision of about 3000. This means that the minimum useful V_{sel} in a 1000 cm^3 object at a 10% level of contamination is about 2 cm^3. With RF pulses designed specifically for high spatial selectivity the spatial precision can be improved by almost an order of magnitude, making the minimum useful voxel , V_{sel}, about 0.3 cm^3. This means that spectra can be obtained from voxels that have linear dimensions of about 6 mm with about a 20 % contamination of outside signal.

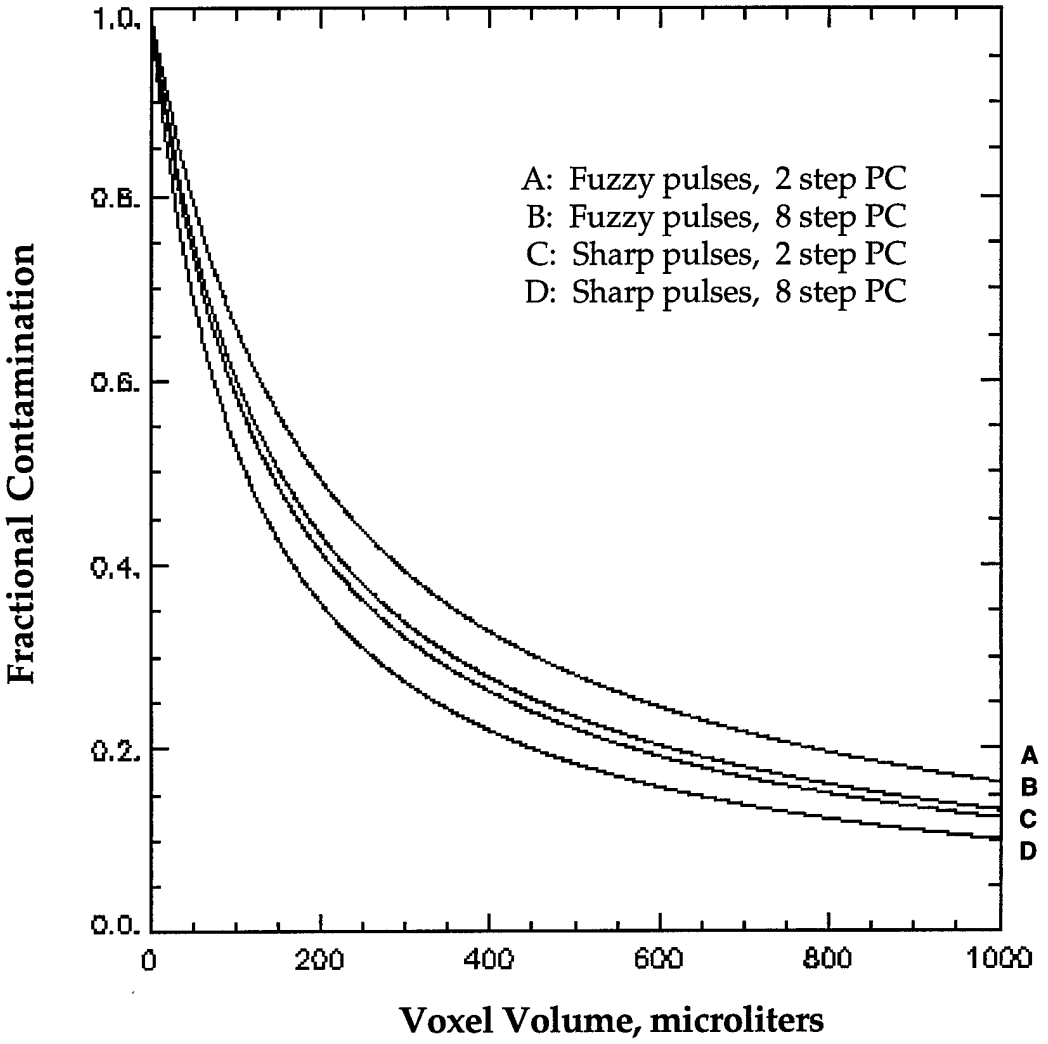

Figure 6. The variation in the fractional level of signal contamination obtained from an analysis of data collected on the phantom shown in Figure 5.

MRS studies of breast lesions at 1.5 T. We have found that it is possible to acquire solvent suppressed proton spectra using the multicoil array described for MRI. The spectra are acquired and stored as four separate data files; one spectrum from each coil. In this mode there are two advantages of the multicoil array over conventional surface coils. The first advantage is that each spectrum has the potential signal-to-noise of a small coil. This feature taken together with the compression of the breast which places the tissue proximal to the coils has meant that we can acquire spectra from structures with volumes of about 0.3 cm^3. The

combined spectra can improve the signal-to-noise of the resultant spectra by as much as $\sqrt{4}$. This extra signal-to-noise results in improved spectral quality and decreased acquisition times. Since we do not know the location of the lesion beforehand the use of the multicoil spectral feature allows us to obtain spectra from each lesion without repositioning of the coil. Typical sets of localized multicoil spectra obtained at 1.5 T are shown in Figures 7, 8, and 9.

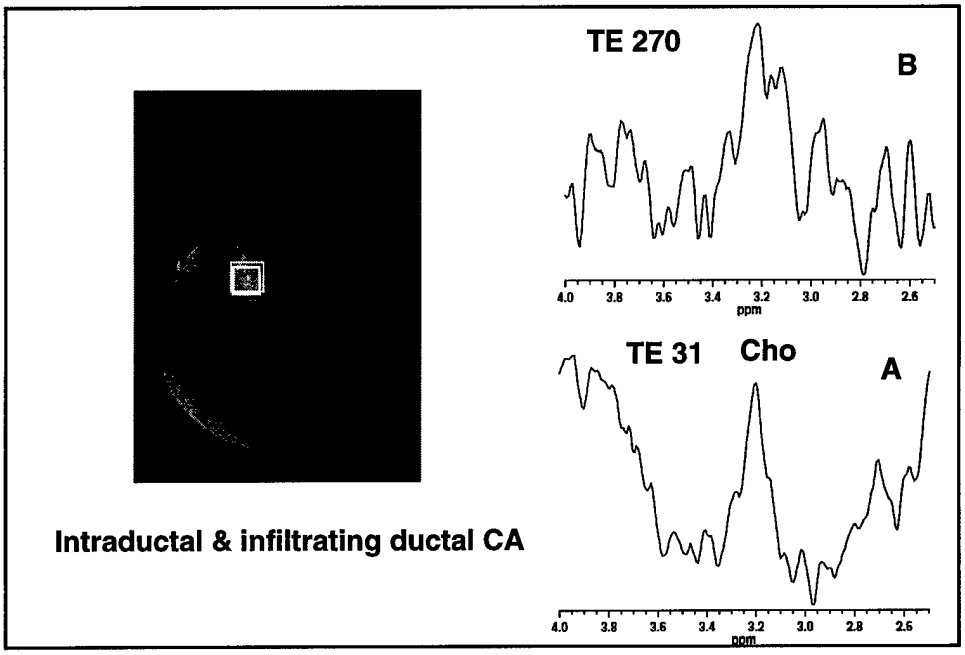

Figure 7. Solvent suppressed proton spectra obtained from a carcinoma. The voxel size was 1 cm by 7 mm by 7 mm. Spectrum A was obtained at a TE of 31 msec. Spectrum B was obtained at a TE of 270 msec.

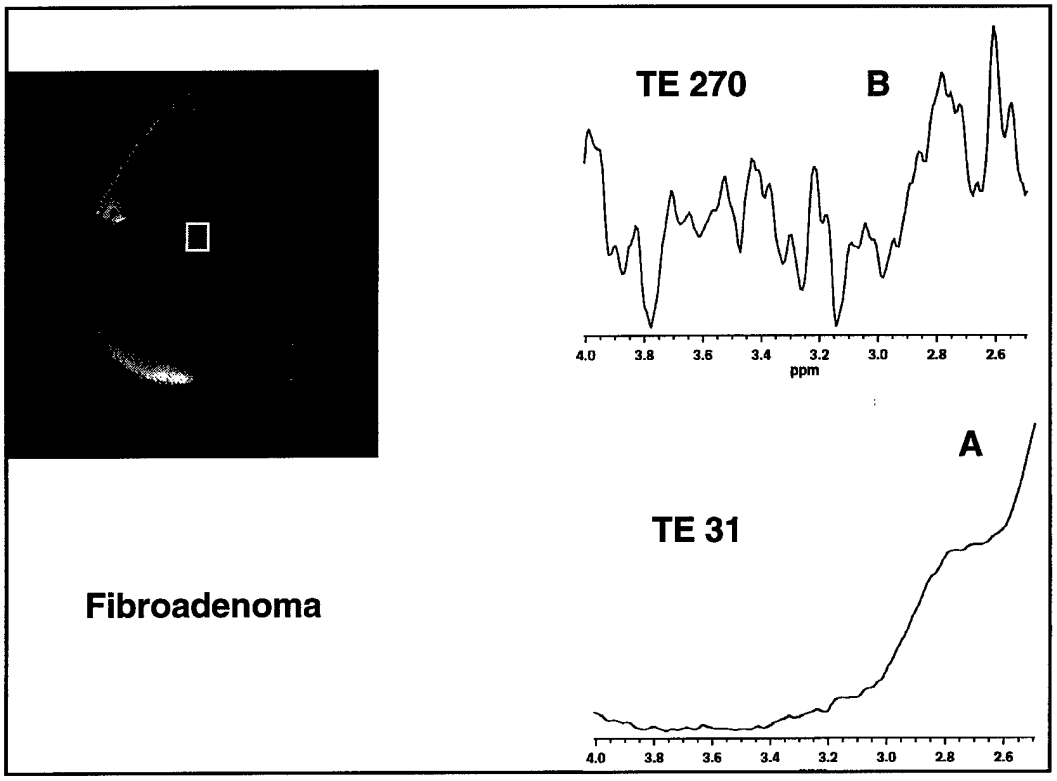

Figure 8. Solvent suppressed proton spectra obtained from a fibroadenoma. The voxel size was 8 mm by 7 mm by 7 mm. Spectrum A was obtained at a TE of 31 msec. Spectrum B was obtained at a TE of 270 msec.

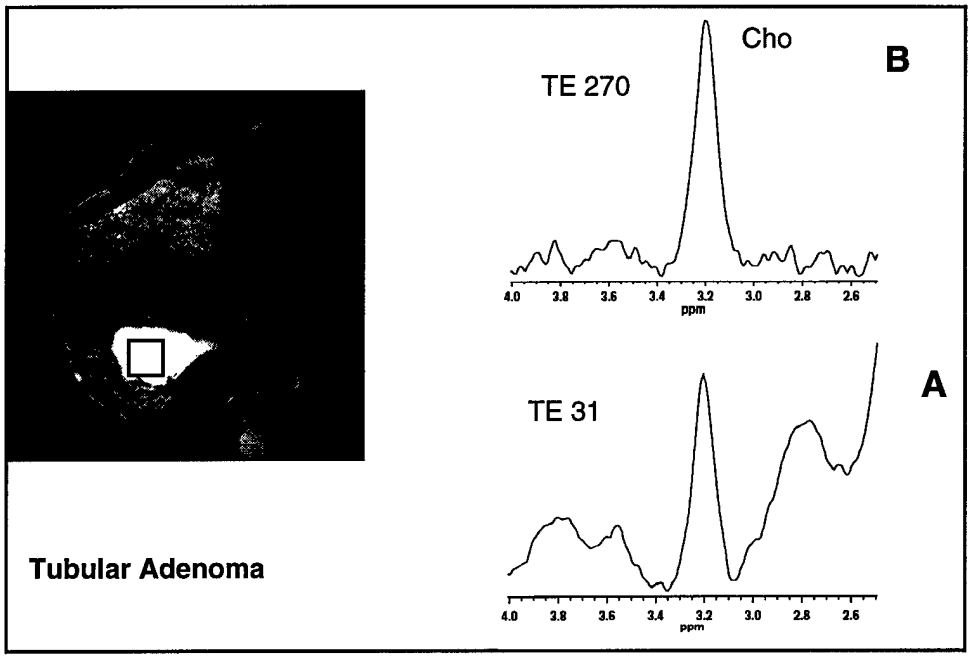

Figure 9. Solvent suppressed proton spectra obtained from a tubular adenoma. The voxel size was 10 mm by 10 mm by 10 mm. The bottom spectrum was obtained at a TE of 31 msec. The top spectrum was obtained at a TE of 270 msec.

The example shown in Figure 9 shows the highest level of choline present in any lesion which we have examined. This lesion which contains very rapidly proliferating epithelial cells is a rare benign mass (this is the only case seen on the breast service this year). It illustrates the importance of combining the MRI features with the MRS data in order to characterize the lesion accurately.

Of the 35 patients enrolled in the MRS study 31 were carried out successfully. The other four cases were uninterpretable due to patient motion. We have analyzed the MRS data obtained on these 31 cases (15 cancers, 16 benign). We have carried out a blinded analysis of the proton MR spectra obtained from these masses to see whether choline can be used to make the distinction between benign and malignant masses. The results obtained are presented in Table 1.

Table 1.

The observation of choline in localized in vivo spectra on patients with focal masses seen on MRI (n=31).

Mass (n=31)	Observation of Choline in the spectrum
Benign (n=16)	1/16
Malignant (n=15)	13/15

Note that choline was observed only in the tubular adenoma shown in Figure 9. The sensitivity of using choline as an indicator for malignancy is 13/15 or 0.87 with a specificity of 15/16 or 0.94. The positive predictive value of using Cho as an indicator of malignancy is 13/14 or 0.93. The negative predictive value is 15/17 or 0.88. These values are extremely encouraging and provide a basis for proceeding with testing this method in a larger cohort. It is likely that the positive predictive value of using Cho as an indicator of malignancy may be higher than that reported above since tubular adenomas are extremely rare lesions.

It is important to evaluate the role of MRS in the context of MRI. To this end we have calculated the sensitivity and specificity of MRI on this same cohort of 31 patients. The sensitivity is 14/15 or 0.93 with a specificity of 0.69. Note that in this cohort all of the lesions observed exhibited some enhancement after injection with Gd-DTPA. This means that we have selected a cohort of patients in which the prevalence of malignancy (0.49) is higher than in a cohort of patients in which non-enhancing lesions are included (0.35). Our collaborators have shown that the negative predictive value of Gd-DTPA enhancement is about 0.97. That is, if a lesion does not exhibit signal enhancement post injection of Gd-DTPA it is almost certainly benign.

We have evaluated two logical combinations of MRI and MRS; the case where both MRI and MRS (MRI+MRS) have to be positive for a lesion to be malignant, and the case where either MRI or MRS (MRI or MRS) is positive for a lesion to be classified as malignant. The sensitivity of MRI + MRS is 0.70 with a specificity of 1.00. The sensitivity of MRI or MRS is 1.00 with a specificity of 0.57. Using these four possibilities we have constructed the ROC curve shown in Figure 10.

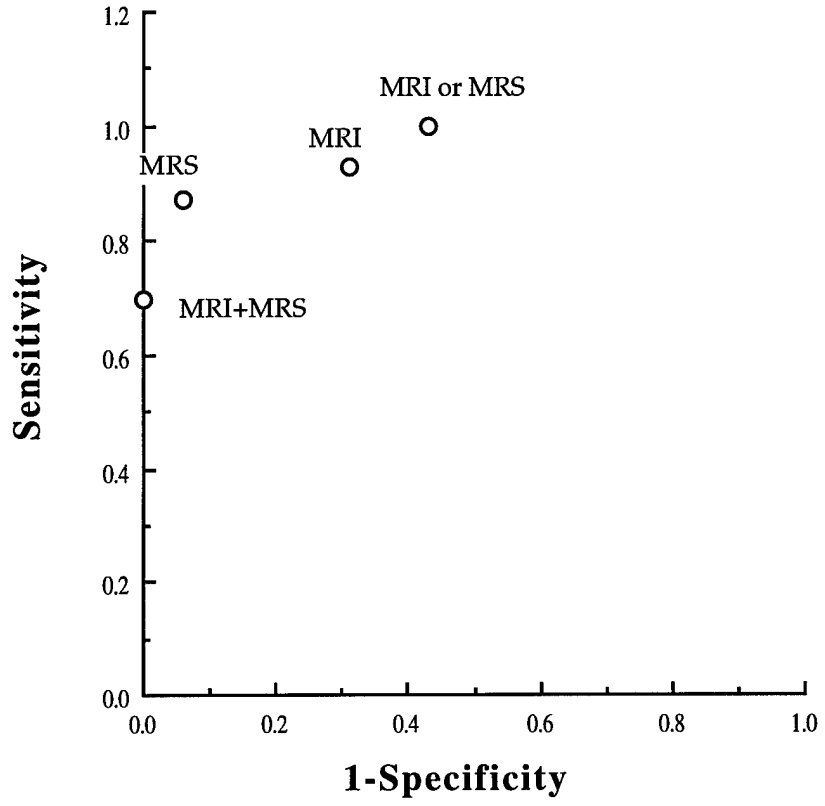

Figure 10. The receiver operator curve constructed from the sensitivities and specificities of the four diagnostic evaluations carried out on the 31 patients who were examined by MRS. The gold standard diagnosis was made based on histopathology.

The results shown in Figure 10 indicate that the combination of MRI+MRS has the highest specificity. The positive predictive value of this combination is 1.00, suggesting that this combination of results can diagnosis malignancy with high certainty.

CONCLUSIONS

We have successfully developed a technical approach that can be employed to produce MRS spectra of the breast lesions as small as $(6\ mm)^3$. These methods have been applied to a cohort of 31 patients. Using the presence of choline in the MR spectra as an indicator of malignancy, the positive predictive value is 0.90. This observation indicates that MRS may be employed in several ways. First it may provide a method for the improved distinction between benign and malignant lesions. Second the presence of choline may provide a means for differentiating recurrent tumor from radiation induced fibrosis. Finally, changes in the choline peak may provide a means for assessing response to therapy in patients with locally advanced breast cancer. Each of these three methods merits further investigation.

In the following sections we present some of our ideas concerning future directions this project may take. These include: 1) MRS studies of breast lesions at 4.0 T, 2) determining the incremental diagnostic efficiency of MRS on a larger cohort of patients, and 3) carrying out an analysis of the cost effectiveness of MRS as a diagnostic method. Each of these is described below.

FUTURE STUDIES

MRS studies of breast lesions at 4.0 T. The recent installation of a 4T research whole body MR scanner in our department offers significant advantages to this project as illustrated below in Figure 11.

We are assessing the advantages of the 4 T scanner (one of only six such scanners operational in the USA) to characterize more extensively spectral abnormalities observed at 1.5 T. Examples of spectra obtained at 4.0 T are shown in Figures 12 and 13.

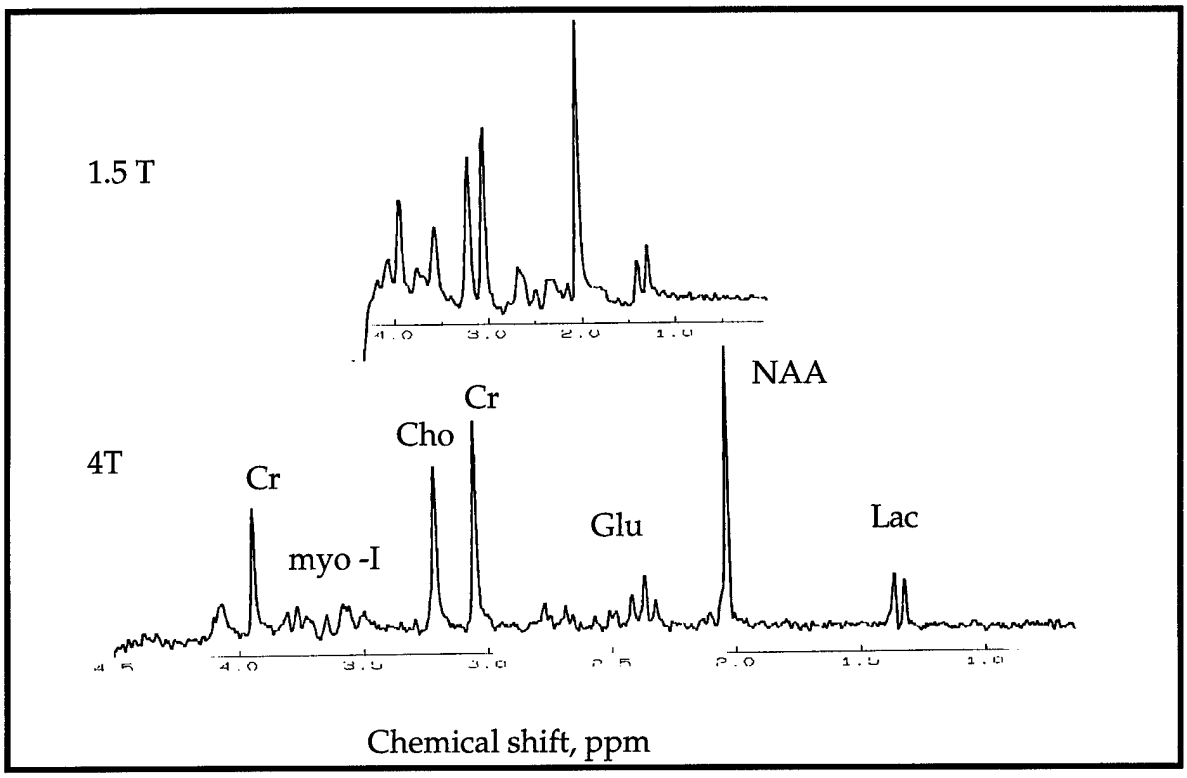

Figure 11. Solvent suppressed proton MR spectra obtained at 1.5 T (top) and 4 T (bottom), of a phantom containing the compounds indicated (Lac is lactate, NAA, Glu is glutamate, Cr is creatine, Cho is choline, myo-I is myo-inositol) plotted on the same frequency scale. The spectra were obtained under identical conditions. There is a factor of 2.67 improvement in chemical shift dispersion at 4 T over 1.5 T.

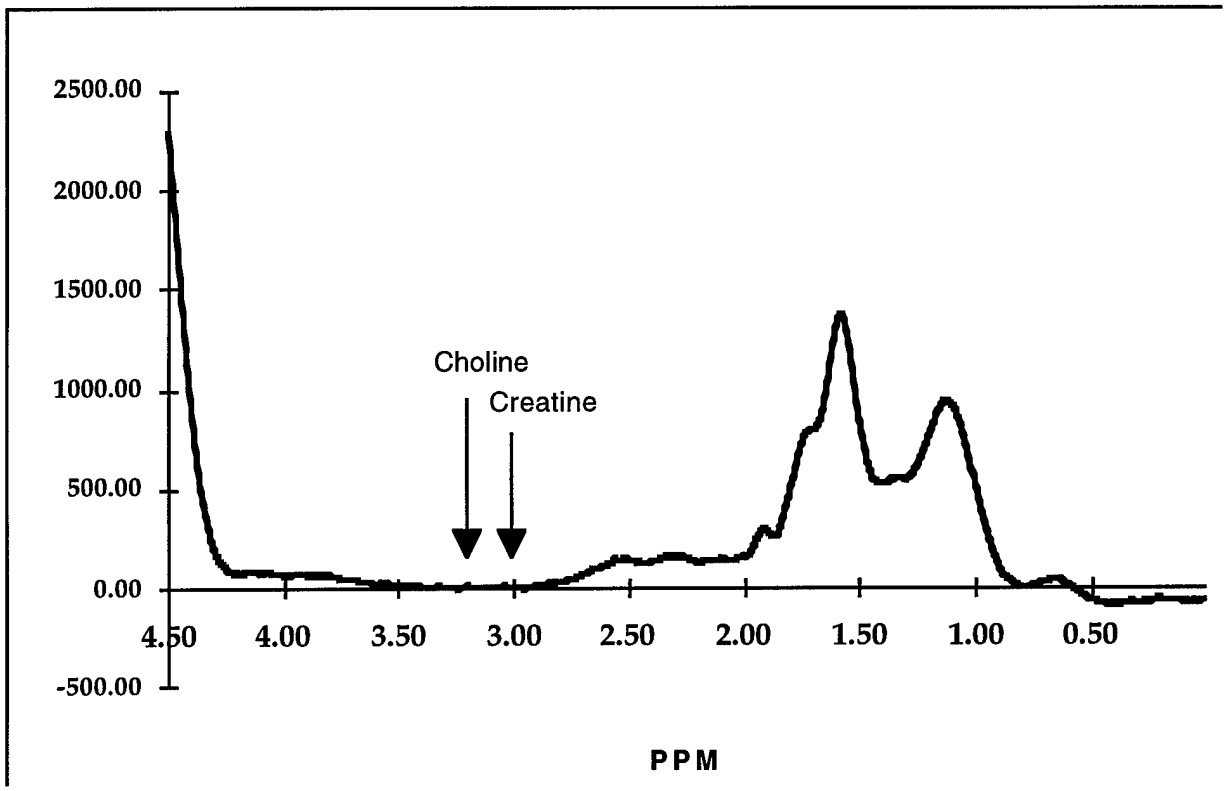

Figure 12. A solvent suppressed proton spectrum obtained from a normal breast tissue at 4.0 T. The voxel size was 10 mm by 10 mm by 10 mm. The spectrum was obtained at a TE of 31 msec using STEAM.

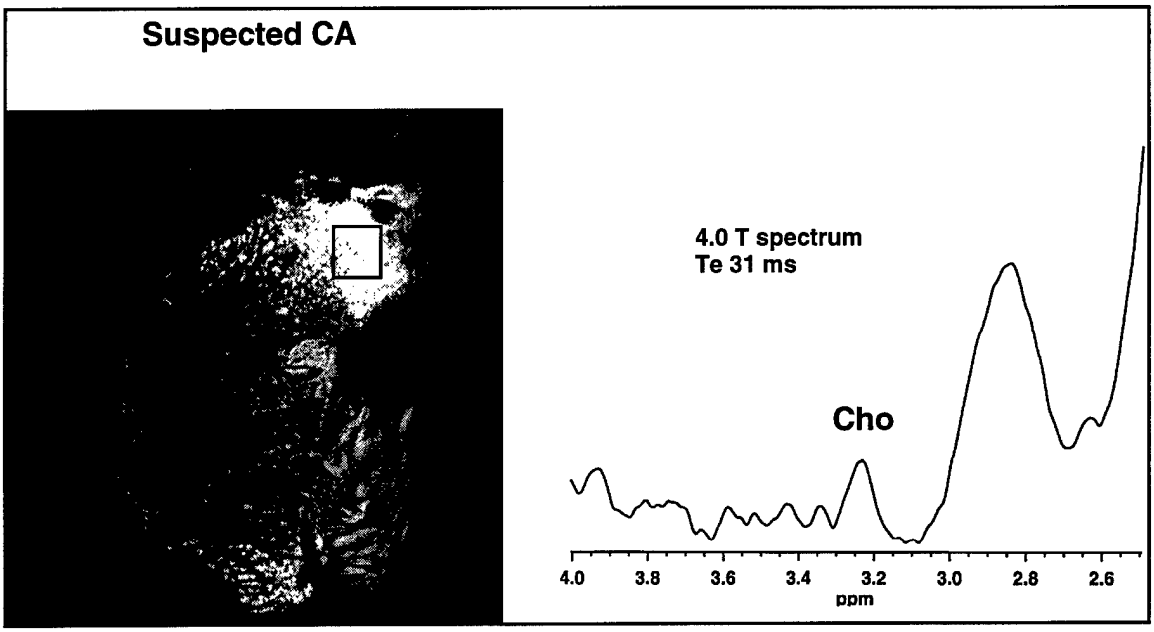

Figure 13. A solvent suppressed proton spectrum obtained from a suspected carcinoma at 4.0 T. The voxel size was 10 mm by 10 mm by 10 mm. The spectrum was obtained at a TE of 31 msec using STEAM.

The example shown in Figure 12 illustrates the advantages of increased chemical shift dispersion of 4.0 T. This dispersion facilitates the detection of choline and creatine as indicated on the spectrum. The observation of choline in the spectrum shown in Figure 13 indicates that the lesion is probably a carcinoma. The examples of 4 T spectra shown demonstrate the advantages of the additional chemical shift dispersion of 4 T over 1.5 T in localized spectra of the breast. However the intent is to employ the 4.0 T data to better understand the MRS results obtained at 1.5 T. The cost and availability of 4 T scanners make it unlikely that MRS of the breast at 4.0 T will become widely used. On the other hand, there is a relatively large installed base of 1.5 T scanners. If as indicated by our results, MRS of the breast has some incremental diagnostic advantage, it would be relatively easy to implement on these scanners making it available to a large group of women.

The evaluation of diagnostic tests. Our department has recently formed a section with a group of investigators who have substantial experience with the

evaluation of diagnostic tests, the modeling of cost effectiveness, and the accounting of costs. Each of these methods may be applied to MRS of the breast. We have begun collaboration with Dr. Curt Langlotz, who is the Chief of the Health Outcomes Research Section in our department to begin to assess MRS of the breast. Dr. Langlotz has recently conducted two studies examining the cost effectiveness of radiological procedures. One study evaluated the cost effectiveness of magnetic resonance angiography (MAR) in the preoperative planning of patients with limb-threatening peripheral vascular disease (55). A second study, evaluated the role of MRI of the prostate gland in preoperative staging of prostatic carcinoma (56). We expect our experience with the construction of cost-effectiveness models, specifically those related to diagnostic tests and procedures, will facilitate the design, construction, and analysis of the decision model for MRS of the breast.

The relevant statistical methods are ROC curves, and tree-structured classification (64). Receiver-operating characteristic curve, so called because of their origin in the early days of radio, are a plot of one minus specificity versus sensitivity. Each point on the plot corresponds to a different choline level used as a cutoff to discriminate between benign and malignant lesions. The point nearest the upper-left corner of the plot may be considered a good cutoff since it maximizes the smaller of sensitivity and specificity; other options include a cutoff that gives good specificity at the trade-off of some degradation in sensitivity. Tosteson and Begg (65) extend the ROC technology to a regression model that can be adjusted for subject-specific variables such as age that can increase precision of estimation without necessarily having diagnostic value.

Tree-structured classification yields an analysis similar in appearance to a corporate organization chart. When several predictors are categorical (e.g., presence/absence or grade of MRI features), compared to logistic regression, the analysis can be more flexible, more easily presented, and statistically superior. The top "node" of the tree might divide women according to choline level; the method can select the cutpoint or use a pre-specified one. Women with extremely high choline levels might constitute a "terminal node"; their chances of a malignancy may be so high that adding more information would be unnecessary. However, a good outcome from this first node might be followed by examination of one or more MRI features that again would yield a split. Modern software for this

technology can choose the split points (a single variable can be split into more than two levels), and choose the variables at each node. Cross-classifying subjects by all levels of all features, with the proportion having a malignancy calculated for each combination, yields a tree with each branch followed as far as possible.

While ROC curve analysis is the best method to compare the performance of diagnostic tests, likelihood ratios offer advantages for optimizing clinical use and impact of diagnostic test results. Thus, likelihood ratios will be derived to translate these results to clinical applicability. The *likelihood ratio* measures the contribution that evidence from a test makes to the probability of an hypothesis--in this case, the probability that advanced disease is present. Likelihood ratios computed for continuous variables provide substantially more diagnostic information than for dichotomous variables. However, the MRI interpretation results will be categorized into one of the five sequential categories from the diagnostic scale used by the image reviewers. These categories will be combined into several groups. Likelihood ratios will be derived for the probability of advanced disease given each MRI result group. This likelihood analysis will serve as an important addition to the dichotomous treatment of MRI by the ROC analysis with particular value for the clinical application of the diagnostic test by physicians. The results will be incorporated into the interactive decision model as described below. Table III of Hanley and McNeil (68), which assumes a one-sided test of significance with alpha=0.05, shows that a sample size N=92 provides 80% power to detect a difference of 0.125 between ROC-curve areas (A_Z). Consequently, a negative result from ROC comparison will be strong evidence against a significant beneficial effect. Although the above methods can easily be generalized to discrimination by multiple peaks, for convenience only one spectral peak (choline) is used for this discussion. With multiple peaks, an ROC curve is generated by a logistic regression with each subject's "score" being the regression-based combination of peak heights. The significance of peak height can be tested within the regression or, with a single marker, by means of 2 x 2 tables (peak high/low x benign or malignant). Tree-structured classification is used to calculate the sensitivity, specificity, PPV and NPV of a spectral decision rule and the increment associated with MRI-based observations. Cross-validation (a feature of the tree-structured software) allows realistic projections of how the diagnostic algorithm can perform with future subjects. Data will be analyzed to assess the

ability of each imaging technique to classify patients correctly into one of two groups: localized or advanced disease. The sensitivity of MRS with and without MRI will be determined by computing the percentage of patients who are correctly identified as having advanced disease. Specificity will be assessed by calculating the percentage of patients with localized disease who are correctly characterized as such. The McNemar chi-square statistic will be used to assess the significance of the difference between proportions (i.e., sensitivities and specificities. ROC curves will be constructed and analyzed using CORROC2 (Charles Metz, University of Chicago).One potential problem in assessing diagnostic performance of MRS using tissue pathology as the reference standard is the issue of verification bias (i.e., that some patients will not undergo biopsy and thus will not have tissue available for pathological conformation of disease stage). Verification bias occurs because such patients are not randomly distributed, but are more likely to involve those patients who are classified as having limited disease (stages A and B). The mathematical method outlined by Greenes and Begg (66) will be used to adjust for verification bias. Performance among different raters will be compared using the kappa statistic (see Fleiss (67), Chapter 13).

The Cost-Effectiveness of MRS. The objective of our cost-effectiveness analysis is to define optimal workup and staging strategies for patients with suspected or confirmed breast cancer. We will construct a decision model that will determine the cost effectiveness of breast MRS with and without MRI for workup and staging. The model will incorporate the results of a comprehensive literature review, the diagnostic accuracy of MRS techniques (from our prospective study), and the cost in a detailed decision-analytic model. The model will include an assessment of the quality of life before and after diagnosis and treatment. The decision model will be used for the following purposes: 1) to analyze and make explicit the trade-offs among safety, efficacy, effectiveness, and cost; and 2) to identify the optimal workup and staging strategies for subgroups of patients with suspected or confirmed breast cancer. We expect our results to show the mammographic and clinical presentations for which breast MRS and/or MRI is indicated prior to histologic diagnosis.

Model Structure. Figure 14 shows the workup algorithm that we will employ in our computer-based decision model. On the basis of mammographic

findings and/or a palpable abnormality, the patient will fall into one of four risk categories. Lesions thought to be definitely benign will undergo routine follow-up mammography. Lesions which are probably benign, but which do not meet all the criteria for benignancy will be placed in a structured short-interval follow-up mammography protocol. Lesions which are definitely or almost definitely malignant will be referred for definitive staging .

Three competing workup strategies will be modeled for those patients whose lesions have suspicious mammographic and/or clinical features that otherwise would result in a referral for surgical biopsy: (1) undergo high-resolution breast MRS with or without MRI, (2) undergo stereotactic core biopsy, and (3) undergo conventional surgical biopsy. Those patients whose lesions who have a benign surgical biopsy will return to routine followup. Those felt to have benign lesions on the basis of MRI or stereotactic biopsy will be referred for short-interval follow-up. Those felt to have suspicious or malignant lesions will be referred for staging and treatment. The predicted differences among the clinical and economic outcomes of these groups of patients will be used as a measure of the cost effectiveness of breast MRI for workup of suspicious lesions.

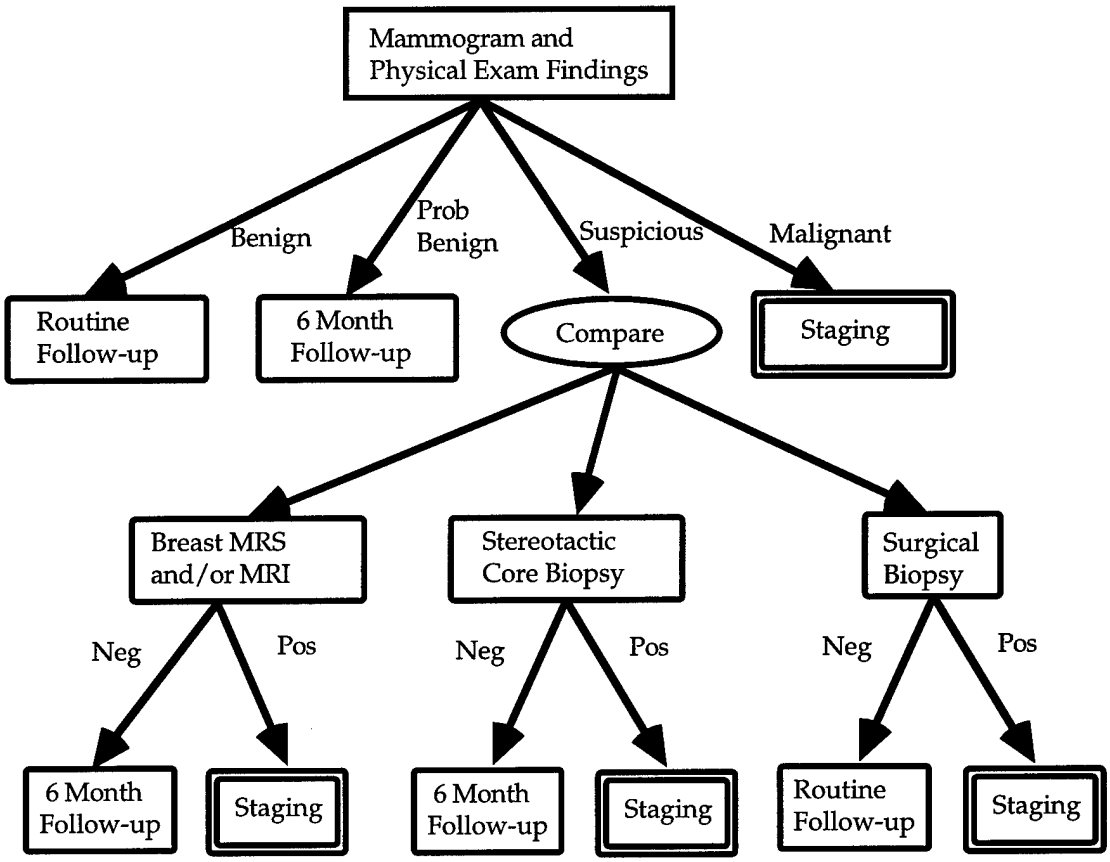

Figure 14: Flow chart demonstrating the workup of breast disease. The detection of an abnormality of mammography or physical exam begins a workup which terminates with follow-up for benign lesions, or staging for malignant lesions. A comparison is made between those patients who are referred for high-resolution MRI, and those who are referred for stereotactic core biopsy. Single rectangles indicate a procedure, test, or protocol. Double rectangles signify the algorithm. Ovals represent a choice.

A decision model will be designed and constructed according to the algorithms shown in Figure 14. The model will be implemented and analyzed using the data from two published models (12, 50) as a starting point. This incremental cost-effectiveness analysis will consider direct medical costs, regardless of who incurs those costs. The model will be stratified by age, clinical presentation, and mammographic appearance. For example, we expect our studies of radiological-pathologic correlation to suggest subgroups of patients whose clinical and mammographic presentation places them in one of three to six categories of risk (e.g., probably benign lesion, indeterminate lesion, probably

malignant lesion, biopsy proven malignant lesion). The measures of cost-effectiveness will be computed and analyzed separately for each of these groups. Each of these decision models will take the form of a conventional decision tree augmented by a Markov process which models various time-dependent parameters such as the clinical course of disease. All viable workup strategies will be considered explicitly: no testing, single tests, and test combinations, including sequential testing strategies.

Modeling Outcomes of Testing. A base case estimate and range of reasonable values will be developed for each parameter in the model. The initial model will be developed and updated according to data from comprehensive, critical literature review and from primary data about the parameter in question. The literature review will identify reported test performance, disease prevalence, outcome probabilities, and patient preferences regarding clinical outcomes. Initial estimates of many parameters can be obtained from the literature, including the diagnostic performance of mammography (5, 69), the proportion of lesions requiring biopsy after 6 month follow-up (14), and the probability of death once diagnosed with breast cancer (70).

When possible, we will estimate parameter values and ranges using information from more than one data source. This technique will allow us to look for consistency among values across data sources. Estimates from these sources will be supplemented by expert estimates when experimental data or reliable published information is not available. A health outcome measure, such as quality-adjusted life years (QALYs) (71), will then be assigned to each branch of the tree. Cost estimates for each diagnosis and management strategy will be obtained the literature (e.g.(12, 53), and from the Medical Resource-based Relative Value Scale (RBRVS) Fee Schedule.

Cost-Effectiveness Results. The results of the cost effectiveness model will be stratified by age and clinical and mammographic presentation, and will be calculated using two basic methods:

1) Cost per surgery avoided. We will develop a cost-effectiveness ratio whereby the incremental cost of each strategy (relative to the baseline strategy) is

the numerator, and the additional cancers detected is the denominator. We will compare these measures of diagnostic value to the use of other tests for particular clinical indications (e.g., PSA screening for prostate cancer).

2) Cost per unit of health outcome. Because many observers prefer more explicit, concrete measures of outcome than the one described above, our second method of integrating cost and effectiveness will combine cost measurements with the equivalent measures of health outcome (e.g., quality-adjusted life years). This calculation will provide a measure of incremental cost per unit of added health outcome that can be compared to other research on the cost effectiveness of medical care interventions (e.g., the cost per quality-adjusted life year offered by coronary bypass grafting, or by mammographic screening).

Sensitivity Analysis. Some model parameters will be subject to several potential biases, including verification bias, changes in referral patterns, and lead-time bias. While these biases will be considered explicitly and attempts will be made to avoid them and to correct for them, standard mathematical correction methods are imperfect (71). It therefore is extremely important to identify the major uncertainties and repeat the analysis under a wide range of parameter values. Accordingly, we will conduct one-way and multi-way sensitivity analyses on the cost-effectiveness model to test the robustness of the model's conclusions. Among the parameters whose sensitivity will be studied in detail are the diagnostic accuracy of breast MRS, the likelihood of complications, and the incidence of breast cancer in the tested population. Such analyses may demonstrate the dependence (or independence) of a result on a particular assumption; they may establish the threshold value of a variable that affects the adoption or rejection of a conclusion; and, they may identify uncertainties that require additional research. Sensitivity analysis may also provide evidence for or against the generalizability of the study to other health care facilities that attract a different patient mix.

We expect the results of our study to yield recommendations regarding the use of the breast MRS for physicians who are contemplating the diagnostic workup of patients with suspected breast malignancy. Because our model is stratified by age, clinical indication, and mammographic appearance, our results will be

expressed in a form usable by clinicians caring for patients with suspicious or malignant breast lesions.

REFERENCES

1. National Institutes of Health Consensus Development Conference Statement:Treatment of Early Breast Cancer. (June 18-21,1990) Bethesda, MD.

2. Adair F, Berg J, Joubert L, et al. Long-term followup of breast cancer patients: the 30 year report. Cancer 1974;33:1145.

3. Behars OH, Shapiro S, Smart C. Report of the working group to review the National Cancer Institute-American Cancer Society Breast Cancer Detection Demonstration Project. J Natl Cancer Inst 1979;62:640-709.

4. Shapiro S, Venet W, Venet L, et al. Ten to fourteen year effect of screening on breast cancer mortality. J Natl Cancer Inst 1982;69(2):349-355.

5. Baker LH. Breast cancer detection demonstration project: five-year summary report. CA 1982;32:194-226.

6. Seidman H, Gelb SK, Silverberg E, et al. Survival experience in the breast cancer detection demonstration project. CA 1987;37:258-290.

7. Feig SA. Decreased breast cancer mortality through mammographic screening: results of clinical trials. Radiology 1988;167:659-665.

8. Tabar L, Fagerberg CJG, Eklund G, et al. Reduction in mortality from breast cancer after mass screening with mammography: first results of a randomized trial in two Swedish counties. Lancet 1985;1:829-832.

9. Verbeek ALM, Hendriks JHCL, Holland R, et al. Reduction of breast cancer mortality through mass screening with modern mammography: first results of the Nijmegen Project. Lancet 1984;1:1222-1224.

10. Martin JE, Moskowitz M, Milbrath JR. Breast cancer missed by mammography. AJR 1979;132:737-739.

11. Hall FM, Storella JM, Silverstone DZ, et al. Nonpalpable breast lesions: recommendations for biopsy based on suspicion of carcinoma at mammography. Radiology 1988;167:353-358.

12. Cyrlak D. Induced costs of low-cost screening mammography. Radiology 1988; 168:661-663

13. Helvie MA, Pennes DR, Rebner M, et al. Mammographic follow-up of low suspicion lesions: compliance rate and diagnostic yield. Radiology 1991;178:155-158.

14. Sickles EA. Periodic mammographic follow-up of probably benign lesions: results in 3,184 consecutive cases. Radiology 1991;179:463-468.

15. Kopans DB. Breast Imaging. Philadelphia: J.B. Lippincott Company 1989.

16. Dowlatshahi K, Yaremko ML, Kluskens LF, et al. Nonpalpable breast lesions:Findings of stereotactic needle-core and fine-needle aspiration cytology. Radiology 1991; 181:745-750.

17. Elvecrog EL, Lechner MC, Nelson MT. Nonpalpable breast lesions: correlation of stereolaxic large-core needle biopsy and surgical biopsy results. Radiology 1993; 188: 453-455.

18. Gisvold JJ, Goellner JR, Grant CS, et al. Breast biopsy: a comparative study of stereotaxically guided core and excisional techniques. AJR 1994; 162: 815-820.

19. Parker SH, Lovin JD, Jobe WE, et al. Nonpalpable breast lesions: Stereotactic automated large-bore biopsies. Radiology 1991; 180:403-407.

20. Harter LP, Curtis JS, Ponto G, et al. Malignant seeding of the needle track during stereotaxic core needle breast biopsy. Radiology 1992; 185: 713-714.19.

21. Sullivan DC. Needle core biopsy of mammographic lesions. AJR 1994; 162: 601-608.

22. El Yousef SJ, Duchesneau RH, Alfidi RJ. Magnetic resonance imaging of the breast. Radiology 1984;150:761-766.

23. Stelling CB, Wang PC, Lieber A, et al. Prototype coil for magnetic resonance imaging of the female breast. Radiology 1985;154:457-462.

24. Dash N, Lupetin AR, Daffner RH, et al. Magnetic resonance imaging in the diagnosis of breast disease. AJR 1986;146-119-125.

25. Kaiser WA, Zeitler E. MR imaging of the breast: fast imaging sequences with and without Gd-DTPA. Radiology 1989;170:681-686.

26. Heywang SH, Wolf A, Pruss E, et al. MR imaging of the breast with Gd-DTPA: use and limitations. Radiology 1989;171:95-103.

27. Stack JP, Redmond AM, Codd MB, et al. Breast disease: tissue characterization with Gd-DTPA enhancement profiles. Radiology 1990;174:491-494.

28. Harms SE, Flamig DP, Hesley KL et al. MR imaging of the breast with rotating delivery of excitation off resonance: clinical experience with pathologic correlation. Radiology 1993; 187:493-501.

29. Boetes C, Barentsz JO, Mus RD, et al. MR characterization of suspicious breast lesions with a gadolinium-enhanced turboFLASH subtraction technique. Radiology 1994; 193: 777-781.

30. Kelcz F, Santyr GE, Mongin et al. Clinical Experience with a Model for Distinguishing Benign from Malignant Breast Lesions Detected with Dynamic Gd-Enhanced MRI. (Abst) RSNA 1994 :89

31. Perman WH, Heiberg EM, Grunz J, et al. A fast 3D-imaging technique for performing dynamic Gd-enhanced MRI of breast lesions. Mag Reson Imag 1994; 12(4): 545-551.

32. Stelling CB, Runge VM, Davey DD, et al Dynamic Enhancement of Breast MRI at 30 Seconds Improves Discrimination of Sclerosisng Adenosis from Invasive Breast Cancer. (Abst) RSNA 1994: 90

33. Weiskoff RM, Hulka CA, Smith B Dynamic NMR imaging of the Breast using Echo-Planar Imaging Book of abstracts: Society for Magnetic Resonsnce in Medicine New York: 1993:119

34. Gilles R, Guinebretiere JM, Lucidarme O, et al. Nonpalpable breast tumors: diagnosis with contrast-enhanced subtraction dynamic MR imaging. Radiology 1994; 191: 625-631.

35. Hickman PF, Moore NR, Shepstone BJ. The indeterminate breast mass: assessment using contrast enhanced magnetic resonance imaging. The British Journal of Radiol 1994; 67: 14-20.

36. vanVaals JJ, Brummer ME, Dixon WT, Tuithof HH, Engels H, Nelson RC, Gerety BM, Chezmas JL, den Boer JA, Keyhole method for accelerating imaging of contrast agent uptake. J Magn Reson Imaging 1993; 3: 671

37. Orel SG, Schnall MD, LiVolsi VA, Troupin RH. Suspicious breast lesions: MR imaging with radiologic-pathologic correlation. Radiology 1994; 190: 485-493.

38. Nunes LW, Orel SG, Schnall MD. Diagnostic accuracy and lesion characteristic predictive values in the MR imaging evaluation of breast masses (abstr). Radiological Society of North America 1994; 267(P): 853

39. Negendank W.Studies of Human Tumors by MRS: A Review. NMR in Biomedicine. 1992; 5: 303-324.

40. Degani H, Ronen SM. and Furman-Haran E. Breast Cancer: Spectroscopy and Imaging of Cells and Tumors. in NMR in Physiology and Biomedicine, Academic Press, NY, 1994, 329-351.

41. Sijens PE, Wijrdeman HK, Moerland MA et al. Human Breast Cancer in Vivo: H-1 and P-31 MR Spectrocopy at 1.5 T. Radiology, 1988;169:615-620.

42. Ng TC, Grundfest S, Vijaykumar S et al. Theerapeutic response of breast carcinoma monitored by ^{31}P MRS in situ. Magn Reson Med, 1989; 10: 125-134.

43. Glasholm J, Leach MO, Collins DJ et al. In-vivo ^{31}P magnetic resonance spectroscopy for monitoring treatment in breast cancer. Lancet, 1989;1: 1326-1327.

44. Smith TA, Glasholm J, Leach MO, et al. A comparison of in vivo and in vitro ^{31}P NMR spectra from humna breast tumours: variations in phopholipid metabolism. Br J Cancer, 1991;63:514-516.

45. Redmond OM, Stack JP, O'Connor NG et al. In vivo phosphorus-31 magnetic resonance spectroscopy of normal and pathological breast tissues. Br J Radiol, 1991;64:210-216.

46. Merchant RE, Thelissen GRP, de Graaf PW et al. ^{31}P magnetic resonance spectroscopic profiles of neoplastic human breast tissues. Cancer Res, 1988;48:5112-5118.

47. Merchant RE, Thelissen GRP, de Graaf PW et al. Clinical magnetic resonance spectroscopy of human breast disease. Invest Radiol , 1991;26:1053-1059.

48. Gribbestad IS, Petersen SB, Fjosne HE et al. ^{1}H NMR Spectrocopic Characterization of Perchloric Acid Extracts from Breast Carcinomas and Non-involved Breast Tissue. NMR in Biomed, 1994;7:182-194.; Gribbestad IS, Fjosne HE, Haugen OA et al. In Vitro Proton NMR Spectroscopy of Extracts from

Human Breast Tumors and non-Involved Breast Tissue. Anticancer Research, 1993;13:1973-1980.

49. Speckter Von H, Blumich B, Just M et al. In-vitro-NMR-Spektroskopie an gesunden, mstopathisch veranderten und karzinomatos befallen Brustdrusengewebsproben, korreliert mit histologischen Befunden. Fortschr Rontgenstr, 1994;161:147-153.

50. Eddy DM, Hasselblad V, McGivney W, and Hendee W (1988). The value of mammography screening in women under age 50 years. JAMA, 1988; 259:1512-1519.

51. Rosenquist CJ and Lindfors KK . Screening mammography in women aged 40-49 years: analysis of cost-effectiveness. Radiology,1994;191::647-50.

52. Smith TJ and Hillner BE. The efficacy and cost-effectiveness of adjuvant therapy of early breast cancer in premenopausal women. J Clin Oncology, 1993;11:771-6.

53. Lindfors KK and Rosenquist CJ. Needle core biopsy guided with mammography: a study of cost-effectiveness. Radiology,1994; 190:217-22.

54. Harms S, Flamig D, Evans W, Harries S, and Bown S. MR imaging of the breast: Current status and future potential. Am J Roentgenol,1994;163:1039-1047.

55. Yin D, Baum RA, Carpenter JP, Langlotz CP, and Pentecost MJ. The cost effectiveness of magnetic resonance angiography in limb-threatening peripheral vascular disease. Radiology, 1995: 194;:757-764.

56. Langlotz C, Schnall M, Tomaszewski J, Malkowicz S, and Schwartz J. The cost effectiveness of endorectal MRI for staging of prostate cancer. Acad Radiol. (In Press), 1995.

57. Tofts PS and Wray S. A Critical Assessment of Methods of Measuring Metabolite Concentrations by NMR Spectroscopy. NMR in Biomed, 1988; 1: 1-10.

58. Thulborn KR and Ackerman JJH. Absolute Molar Concentrations by NMR in Inhomogeneous B_1. A Scheme for Analysis of in vivo Metabolites. J Magn Reson, 1983; 55:357-371.

59. Li S-J, Wehrle JP, and Glickson JD. Measurement of the Absolute in vivo Phosphorus Metabolite Concentrations by $^{1}H/^{31}P$ NMR Spectroscopy: Applications to Subcutaneous RIF-1 Tumors. SMRM Abstracts,1988; 2:825.

60. Kreis R, Ernst T, and Ross BD. Absolute Concentrations of Water and Metabolites in Human Brain. II Metabolite Concentrations. J Magn Reson Ser B,1993; 102:9-19.

61. Abragam A, Principles of Nuclear Magnetism. Oxford University Press, Oxford 1961.

62. Wehrli FW, Breger RK, MacFall JR, Daniels DL, Haughton VM, Charles HC, Williams AL. Quantification of contrast in clinical MR brain imaging at high field. Investigative Radiology,1985; 20: 3690-369.; Wehrli FW, MacFall Jr, Glover GH, Grigsby N, Haughton VM, Johnson J, The dependence of Nuclear Magnetic Resonance Image contrast on Intrinsic and pulse sequence timing parameters. Magnetic Resonance Imaging. 1984; 2; 3-16. ;Wehrli FW, MacFall JR, Shutts D, Breger RK, Herfkens RJ. Mechanisms of contrast in NMR imaging. J Computer Assisted Tomography, 1984; 8:369-380.

63. Insko EK and Bolinger L. Mapping of the Radio frequency Field. J Magn Reson Ser A, 1993; 103: 82-85.

64. Breiman L, Friedman J, Olshen R, Stone C. Classification and Regression

Trees, 1984, Wadsworth: Belmont, California.

65. Tosteson AA, Begg CB A general regression methodology for ROC curve estimation. Medical Decision Making, 1988; 8; 204-215.

66. Greenes RA and Begg CB. Assessment of diagnostic technologies: Methodology for unbiased estimation from samples of selectively verified patients. Investigative Radiology,1985; 20:751-756.

67. Fleiss J, Statistical Methods for Rates and Proportions. 2nd ed. 1981, New York: John Wiley and Sons.

68. Hanley J and McNeil B. The meaning and use of the area under a receiver operating characteristic (ROC) curve. Radiology, 1982; 143:29-36.

69. Bassett LW, Liu TH, Giuliano AE, and Gold RH. The prevalence of carcinoma in palpable vs impalpable, mammographically detected lesions. AJR,1991; 157:21-24.

70. Commerce USDo, Vital statistics: Statistical abstract of the United States. 11th ed. 1991, Washington, D.C.: U.S. Government Printing Office.

71. Pliskin JS, Shepard DS, and Weinstein MC. Utility functions for life years and health status. Operations Research, 1980; 28:206-224.

Abbreviations Employed in the Text.

MRI Magnetic Resonance Imaging
MRS Magnetic Resonance Spectroscopy
Gd-DTPA Gadolinium(III) diaethylene-triamine-pentaacetic acid
2D two dimensional
3D three dimensional
Gd Gadolinium
PME phosphomomester
PDE phophodiester
Cho choline
NMR Nuclear Magnetic Resonance
ATP adenosine triphosphate
C-13 carbon-thirteen
PCr phosphocreatine
GPC glycerol phosphorylcholine
TP true positive
FN false negative
TN true negative
FP false positive
PPV positive predictive value
NPV negative predictive value
T1 spin lattice relaxation time
T2 spin spin relaxation time
FSE fast spin echo
MR Magnetic Resonance
STEAM stimulated echo acquisition mode
TR repetition time
TE inter-echo delay
FID free induction decay
CSI chemical shift imaging
SNR signal to noise
RF radio frequency
NAA N-acetylaspartate
CHESS chemically shift selective
PC phase cycling

BIBLIOGRAPHY

Abstracts:

To Be Presented at the International Society of Magnetic Resonance in Medicine , New York, April 26-30, 1996

Proton Magnetic Resonance Spectroscopy of Human Breast at 4.0 T.

J.R. Roebuck, R.E. Lenkinski, L. Bolinger and M.D. Schnall. Hospital of The University of Pennsylvania, Philadelphia.

Spatially Localized Proton Magnetic Resonance Spectroscopy of Human Breast Disease at 1.5 T.

J.R. Roebuck, R.E. Lenkinski and M.D. Schnall. Hospital of The University of Pennsylvania, Philadelphia.

Submitted to the Radiologic Society of North America, Chicago Illinois, Dec. 1-6, 1996

Characterization of Human Breast Lesions Using Proton Magnetic Resonance Spectroscopy

J.R. Roebuck, R.E. Lenkinski, David B. Clayton and M.D. Schnall. Hospital of The University of Pennsylvania, Philadelphia.

List of Personnel supported by the Contract

Names	Degree	Role on Project	Percent Effort
Robert Lenkinski	Ph.D.	Principal Investigator	20%
Lawrence Solin	M.D.	Co- Investigator	10%
Mitchell Schnall	M.D.	Co- Investigator	20%
Susan Orel	M.D.	Co- Investigator	20%
Peter Bloch	Ph.D.	Co- Investigator	10%
McDermott	R.N.	Nurse Cordinator	100%
Tim Allman	Ph.D.	Post-Doc Fellow	100%
Yoram Rubin	Ph.D.	Post-Doc Fellow	100%
Kim Cecil	Ph.D.	Post-Doc Fellow	100%
Edith Wilkins		Administrative Assistant	10%